International Journal of
Translational Medicine

MDPI

Article

CD34-Stained Microvessel Density and Immune Checkpoint Inhibitor Outcomes in Metastatic Non-Squamous Non-Small Cell Lung Cancer: A Retrospective Study

Emir Cerme [1], Sebnem Batur [2], Cansu Yol [3], Eray Ontas [4], Akif Turna [5], Ayşim Büge Öz [2] and Zeynep Hande Turna [1,*]

[1] Division of Medical Oncology, Department of Internal Medicine, Cerrahpaşa Faculty of Medicine, Istanbul University-Cerrahpaşa, 34098 Istanbul, Türkiye; emircermemd@gmail.com (E.C.)
[2] Department of Pathology, Cerrahpaşa Faculty of Medicine, Istanbul University-Cerrahpaşa, 34098 Istanbul, Türkiye; batursebnem@gmail.com (S.B.); ozbuge@gmail.com (A.B.Ö.)
[3] Memorial Sloan Kettering Cancer Center, Department of Pathology and Laboratory Center, New York, NY 10065, USA; cansu61yol@gmail.com
[4] Division of Epidemiology, Department of Public Health, Faculty of Medicine, Ankara University, 06230 Ankara, Türkiye; eontas@ankara.edu.tr
[5] Department of Thoracic Surgery, Cerrahpaşa Faculty of Medicine, Istanbul University-Cerrahpaşa, 34098 Istanbul, Türkiye; akif.turna@gmail.com
* Correspondence: hturna@iuc.edu.tr; Tel.: +90-212-414-30-00

Abstract

Background/Objectives: Immune checkpoint inhibitors (ICIs) improve outcomes in metastatic non-squamous non-small cell lung cancer (NSCLC), yet predictive biomarkers remain limited. This study investigated whether CD34-stained microvessel density (MVD) is associated with ICI efficacy. Methods: Patients with metastatic non-squamous NSCLC and tumor specimen suitable for anti-CD34 immunohistochemistry were included. In the derivation cohort, ROC analysis for objective response rate (ORR; CR + PR) identified a Youden-optimized threshold of 14.5 vessels/HPF (×400) (sensitivity 67%, specificity 93%; AUC 0.744, 95% CI 0.53–0.95; $p = 0.021$), which was applied without re-optimization to an internal validation cohort and a chemotherapy-only comparator. Results: In the derivation cohort, ($n = 25$), ORR was higher with MVD $\geq$ 14.5 than <14.5 (88.9% vs. 25.0%; $p = 0.004$) and OS/TFST were longer (OS: 53.0 vs. 17.1 months, $p = 0.037$; TFST: 50.0 vs. 6.0 months, $p = 0.014$). In the validation cohort ($n = 13$), MVD $\geq$ 14.5 was associated with longer TFST (9.0 vs. 4.0 months; $p = 0.035$) and numerically longer OS (12.0 vs. 7.0 months; $p = 0.059$). As a cut-off-independent sensitivity analysis, continuous MVD (per five vessels/HPF) was associated with longer TFST (HR 0.663, 95% CI 0.454–0.969; $p = 0.034$). No association was observed in the chemotherapy-only cohort. Conclusions: Higher CD34-MVD may be a feasible vascular metric associated with ICI outcomes that warrants prospective validation.

Keywords: microvessel density; CD34; angiogenesis; immune checkpoint inhibitor; non-small cell lung cancer

Check for updates

Academic Editor: Ewa Grzybowska

Received: 5 March 2026
Revised: 12 April 2026
Accepted: 16 April 2026
Published: 20 April 2026

Copyright: © 2026 by the authors. Licensee MDPI, Basel, Switzerland. This article is an open access article distributed under the terms and conditions of the Creative Commons Attribution (CC BY) license.

1. Introduction

Lung cancer is one of the leading causes of cancer-related mortality [1]. NSCLC accounts for approximately 85% of newly diagnosed lung cancer, with adenocarcinoma and squamous cell carcinoma being the most common histologic types [1,2]. Since diagnosis is usually made at later stages, new treatment approaches for advanced-stage NSCLC have been incorporated into daily practice over the years [2–7].

ICIs have been the standard treatment for advanced-stage NSCLC [3–7]. These agents are PD-1 inhibitors nivolumab and pembrolizumab; the PD-L1 inhibitors atezolizumab, durvalumab, and avelumab; and the CTLA-4 inhibitor ipilimumab [3,4,8–11]. Treatment strategies in metastatic NSCLC comprise anti-PD-1/PD-L1 monotherapy in PD-L1-high tumors; chemo-immunotherapy combinations, anti-PD-1/PD-L1 plus anti-CTLA-4 regimens [4,7–11]. There are multiple factors that limit ICI efficacy. These are primary and acquired resistance, oncogenic co-alterations, non-inflamed phenotype of tumor microenvironment (TME), suboptimal predictive performance of PD-L1 expression, and immune-mediated adverse events [12–14]. Moreover, based on real-life experiences, there could be some differences from phase 3 trials, possibly due to the more flexible criteria for patient selection in the real world.

PD-L1 expression has emerged as a predictive biomarker for ICI efficacy [3–5,7]. However, PD-L1 status may exhibit intratumoral heterogeneity, and the results can be influenced by interventions such as radiotherapy [3–5,7]. Thus, further studies are warranted to define biomarkers for predicting ICI efficacy, with the aim of identifying the most appropriate candidates who may benefit from these agents.

TME has become a field of work to explore the relationship between tumor cells and immune cells [15–20]. Interactions between tumor cells and the immune system may trigger various mechanisms, both pro-inflammatory and anti-inflammatory [15–17,21–24]. Increased angiogenesis is a result of interactions between immune cells, tumor cells, and stromal elements in tumor tissue [15,24,25]. Vascular endothelial growth factor (VEGF) and angiopoietins are the main regulators of tumor angiogenesis [15,24,26,27], which is characterized by leaky and fragile vessels [25–28]. Moreover, these growth factors inhibit effector T lymphocytes and upregulate PD-1, LAG-3, and TIM-3 on the lymphocyte surface [15,24,25]. VEGF-mediated angiogenesis was shown to contribute to tumor cell survival [18,26–28], creating a hypoxic microenvironment that precedes the activity of immune cells [18,24,25,29]. Additionally, it increases the accumulation of immunosuppressive cells (M2 tumor-associated macrophages, regulatory T lymphocytes, MDSCs, etc.) in tumor tissue [17,24,25].

On the other hand, vascular normalization in tumor tissue, described as amelioration of vessels with adequate pericyte coverage, may reverse this effect and provide delivery of antitumoral immune cells, enhancing ICI efficacy [30,31]. Vascular normalization can be achieved either using targeted drugs or spontaneously (genetically driven) [32,33]. In previous studies, investigators used immunohistochemistry (IHC)-based endothelial labeling (e.g., CD31 or CD34) in combination with pericyte markers as an approach to determine vascular normalization [34–37].

Tumoral MVD is a histologic estimate of the endothelial compartment obtained by IHC on routine FFPE tissue [38–40]. MVD primarily measures vessel abundance, depending on anatomic site and hotspot selection and does not capture pericyte coverage or perfusion which are the essential findings of vascular normalization [39,40]. MVD has been commonly measured using IHC-based CD31, CD34, and CD105 staining in previous studies [27,38,39,41,42]. Increased MVD count was found to be associated with worse overall survival in some previous studies [27,29,38,41,43,44], although contradictory results were reported, potentially due to differences in assessment methods [40,45]. CD34 is widely used in lung cancer because it sensitively highlights microvessel structures, allows reproducible hotspot counting, and has demonstrated prognostic associations in NSCLC cohorts [38]. However, there is a lack of evidence suggesting the role of MVD alone to assess ICI efficacy.

This study investigated whether CD34-stained microvessel density (MVD) is associated with ICI efficacy in metastatic non-squamous NSCLC.

2. Materials and Methods

2.1. Study Population

We retrospectively searched data of patients with metastatic non-squamous NSCLC between January 2017 and March 2025. Three cohorts were analyzed: derivation cohort (primary analysis), non-overlapping internal validation cohort, and chemotherapy-only comparator arm. Cohorts were separated by treatment era reflecting evolving practice changes. In the earlier period, ICIs were predominantly administered in the second-line setting, whereas in the later period ICIs became standard in the first-line setting. The patient selection flowchart is shown in Figure 1.

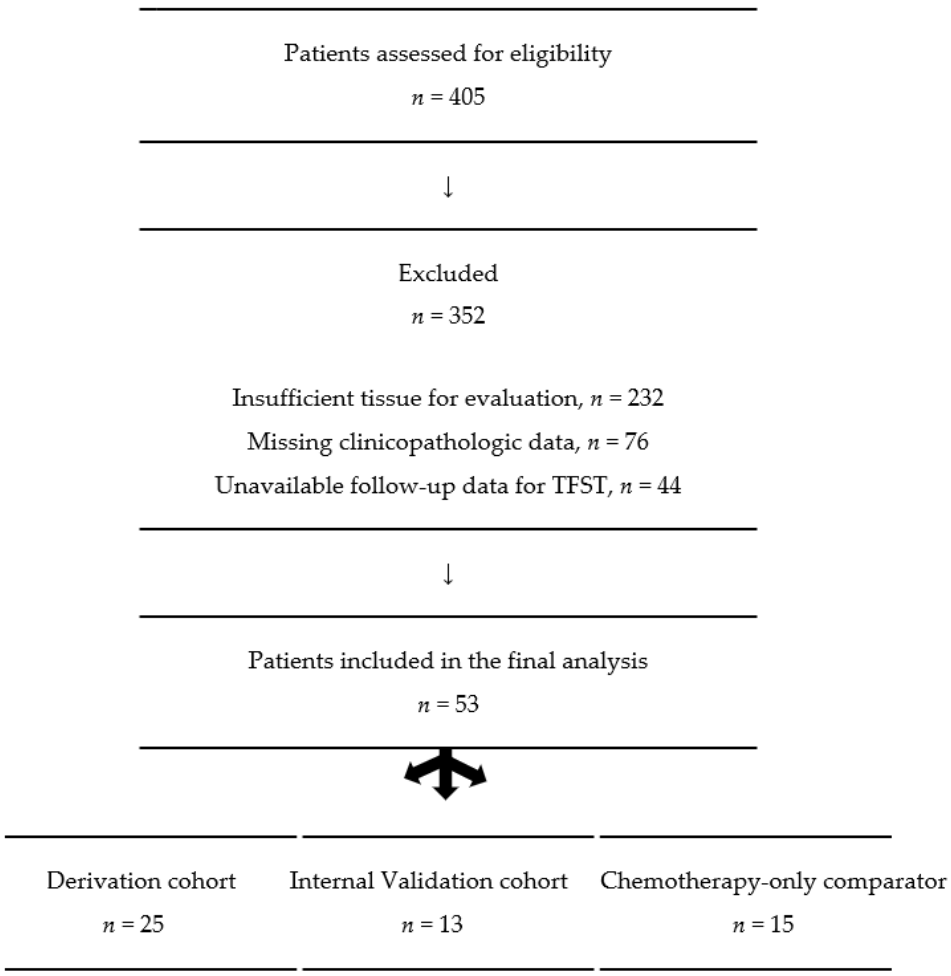


Figure 1. Patient selection flowchart.

The study was conducted in accordance with the Declaration of Helsinki and approved by the Clinical Research Ethics Committee of Istanbul University-Cerrahpasa Faculty of Medicine (ID: 89403766-604.01.02.9846, approval date 6 March 2025) for studies involving humans.

IHC staining for Epidermal Growth Factor Receptor (EGFR), Anaplastic Lymphoma Kinase (ALK), and ROS1 were negative for all patients. Resection materials regarding primary tumors and regional lymph nodes were evaluated by an expert pathologist to assess their convenience for IHC by hematoxylin eosin staining. Eligibility required the availability of a formalin-fixed, paraffin-embedded (FFPE) tumor tissue block adequate for immunohistochemistry and MVD assessment. Cases with diagnosis established by fine needle aspiration (FNA) or cytology without an adequate tissue block were excluded. Specimens included tru-cut biopsies and surgical resections (wedge resection, lobectomy,

pneumonectomy). The derivation cohort (n = 25) included patients treated with ICIs who had a FFPE tumor tissue block suitable for anti-CD34 IHC. A non-overlapping internal validation cohort (n = 13) represented ICI-treated patients meeting the same eligibility criteria. The MVD cut-off derived in the primary analysis was applied without re-optimization. The chemotherapy-only comparator arm (n = 15) covered patients receiving chemotherapy without ICIs who met the same tissue eligibility criteria.

Response rates were evaluated using computed tomography (CT) scans according to Response Evaluation Criteria in Solid Tumors (RECIST) version 1.1. For ICI-treated patients, iRECIST criteria were used to account for atypical response patterns. Fluorodeoxyglucose positron emission tomography (FDG-PET CT) was considered supportive for clinical interpretation. Objective response rate (ORR) was considered as having a complete response or partial response. Follow-up imaging was performed using the same modality as at baseline. Overall survival (OS) and time to first subsequent therapy (TFST) were determined. OS was defined as the time interval between initiation of ICIs and death, while TFST was defined as the time from ICI initiation to start of the new first subsequent systemic therapy. Continuation of ICI was permitted for patients with oligoprogression, which is amenable to local therapies.

2.2. Biomarker Assessment

Tumor specimens were fixed in formalin and then embedded in paraffin. Sections were dewaxed in xylene, rehydrated through graded alcohols, and incubated in 3% hydrogen peroxide for 10 min at room temperature. After washing with phosphate-buffered saline (PBS) (pH = 7.6) for 5 min, the sections were incubated in citrate buffer (pH = 6) for 15 min. The specimens were rinsed in distilled water. The sections were processed with a protein-blocking step for 20 min prior to incubation with primary antibodies. The sections were incubated for two hours at room temperature with an anti-CD34 monoclonal antibody (monoclonal mouse anti-human CD34 class II clone QBEnd 10 ready-to-use/DAKO, Glostrup, Denmark). Then, the sections were rinsed in PBS and incubated at room temperature for 20 min with secondary antibodies (multi-species ultra-streptavidin detection system-HRP; Signet, Norwell, MA, USA). Sections were rinsed in PBS and incubated in streptavidin–biotin complex for 30 min. Sections were rinsed in PBS, then developed with diaminobenzidine tetrahydrochloride (DAB) for 10 min and counterstained with hematoxylin. Sections were dehydrated through graded alcohols of 90%, 95%, and 99.9%, respectively, for 5 min each. IHC staining was performed on a fully automated Benchmark XT Slide Stainer (Ventana Medical Systems, Tucson, AZ, USA).

At least two areas for each specimen were analyzed by two expert pathologists who were blinded to clinical outcomes. Histopathologic assessment was performed using an Olympus bright-field light microscope. The most intense two regions of neovascularization, referred to as "hotspots," were identified under low microscopic power (×40). At hotspots, all CD34-stained vessels were recounted at ×400 magnification, excluding vessels with muscular walls and necrosis areas (Figure 2). MVD was identified as vessels per high-power field (HPF) at ×400 total magnification, and the area was approximately 0.196 mm^2. The mean count of two fields was recorded as MVD score. A formal Weidner scoring system was not applied. Conflicts between the two pathologists were resolved by an independent third pathologist. For PD-L1 staining, the 22C3 pharmDx [Dako, Carpinteria, CA, USA] and the OptiView DAB IHC detection kit were used.

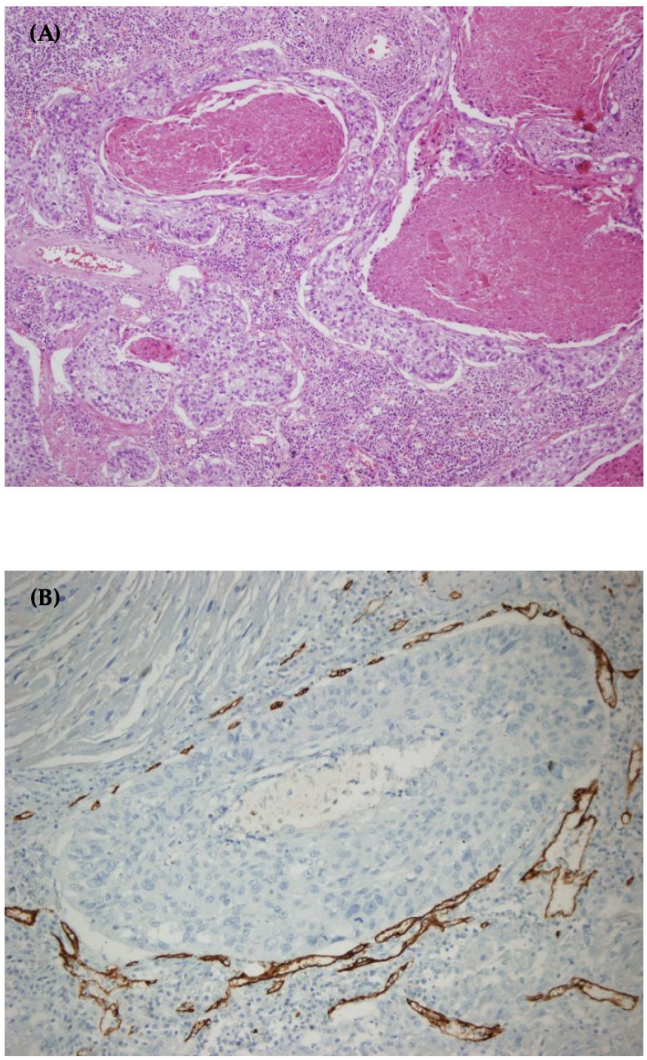


Figure 2. CD34-stained microvessel density in a lobectomy specimen. (**A**) Hematoxylin eosin staining for the specimen (×100 magnification); (**B**) CD34-stained areas (×200 magnification).

2.3. Statistical Analysis

Statistical analyses were performed using IBM SPSS version 30 (IBM Corp., Armonk, NY, USA). ROC curve analysis was used to assess the relationship between MVD scores and ORR. TFST and OS were analyzed in derivation, validation and comparator cohorts using the Kaplan–Meier method, and survival curves were compared with the log-rank test. Cox proportional hazards regression was used to estimate hazard ratios (HRs) with 95% confidence intervals (CIs) for associations between variables and survival outcomes.

To reduce reliance on a single dichotomous threshold, MVD was modeled both categorically and as a continuous predictor. For continuous modeling, MVD was expressed as MVD_5 (per 5 vessels/HPF increase) to improve interpretability of effect estimates. Continuous and categorical MVD models were put in separate regression models to avoid collinearity.

Because of limited event numbers, multivariable models were prespecified to be parsimonious, prioritizing clinically relevant covariates, and the results were interpreted as exploratory where appropriate. To assess the stability of regression estimates under small-sample conditions, bootstrap resampling was performed for Cox models using 2000 bootstrap samples and bias-corrected and accelerated (BCa) 95% CIs.

To evaluate whether the association between MVD and outcomes varied by another factor (effect modification), interaction analyses were performed by including multiplicative interaction terms (MVDxPD-L1 and MVDxtreatment type) in Cox models (for TFST/OS) and logistic regression (for ORR). For continuous interactions, MVD_5 was mean centered prior to creating interaction terms to improve interpretability.

Given missing PD-L1 data in a subset of patients, PD-L1-adjusted analyses were conducted as sensitivity analyses limited to the ICI-treated population (validation + derivation cohort). All p values were two-sided, and $p < 0.05$ was considered statistically significant.

3. Results

Fifty-three patients with metastatic non-squamous NSCLC were included, comprising 25 patients in the derivation cohort, 13 in the internal validation cohort, and 15 in the comparator arm. The characteristics of the derivation cohort are presented in Table 1. In this cohort, 15 patients were aged <65 years, and 10 patients were aged ≥65 years. Six patients had brain metastasis at diagnosis. All patients were treated with anti-PD-1 agents.

Table 1. The characteristics of the derivation cohort (n = 25).

Characteristic	n (%)
Median age (range)	63 (39–80)
Sex	
Male	20 (80%)
Female	5 (20%)
Smoking Status	
Heavy smoker (≥30 pack-years)	14 (56%)
Light smoker (<30 pack-years)	8 (32%)
Non-smoker	3 (12%)
Number of Metastatic Sites	
1 site	16 (64%)
2 sites	7 (28%)
≥3 sites	2 (8%)
Line of ICI Therapy	
First-line	9 (36%)
Second-line	16 (64%)
ICI Used	
Nivolumab	21 (84%)
Pembrolizumab	4 (16%)

In the derivation cohort, seven patients had undergone surgery before starting ICI therapy. Of these, six underwent lobectomy, and one underwent pneumonectomy. Two of these seven patients had oligometastatic disease, whereas five experienced disease progression within 6 months after the adjuvant period and received ICI as first-line treatment. Tumor characteristics of the derivation cohort are described in Table 2.

ROC analysis was performed in the derivation cohort to evaluate the ability of tumoral MVD to discriminate ORR from non-responders. The Youden-index-optimized threshold was 14.5 vessels/HPF (×400), yielding 67% sensitivity and 93% specificity (AUC = 0.744; 95% CI: 0.53–0.95; p = 0.021; Figure 3), indicating moderate discrimination. This fixed, data-derived threshold was then applied without re-optimization to stratify subsequent OS and TFST analyses. These cut-off-based survival comparisons in the derivation dataset were interpreted as exploratory. Internal resampling validation of the Youden-selected ROC cut-off (bootstrapping) was not performed.

Table 2. Tumor characteristics of the derivation cohort (n = 25).

Characteristic	n (%)
PD-L1 expression	
<1%	9 (36%)
1–49%	3 (12%)
≥50%	5 (20%)
Missing	8 (32%)
Histology	
Adenocarcinoma	20 (80%)
NSCLC, NOS	5 (20%)
Specimen Obtained By	
Tru-cut biopsy	16 (64%)
Wedge resection	2 (8%)
Lobectomy	6 (24%)
Pneumonectomy	1 (4%)

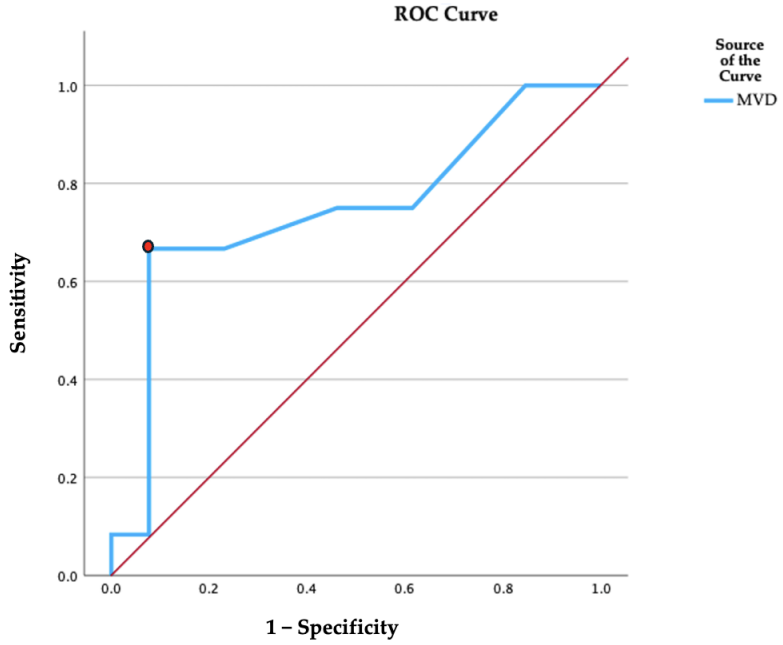


Figure 3. ROC curve of microvessel density (MVD) score for predicting objective response rate (ORR). The diagonal red line represents the line of no discrimination (AUC = 0.5). The red spot indicates the cut-off value of MVD as 14.5. (AUC = 0.744, 95% CI: 0.53–0.95).

In the derivation cohort, ORR was 88.9% (95% CI 56.5–98.0) for MVD ≥ 14.5 vs. 25.0% (95% CI 10.2–49.5) for MVD < 14.5 (Fisher's exact, p = 0.004). The absolute risk difference was 0.64 (95% CI: 0.07–0.88), corresponding to a relative risk (RR) of 3.56 (95% CI: 1.47–8.56). On univariable logistic regression, MVD ≥ 14.5 was associated with higher odds of response (OR = 23.8; 95% CI: 2.25–250; p = 0.008).

In the derivation cohort, OS was significantly longer in cases with MVD ≥ 14.5 (53 months, 95% CI: 11.4–94.7), compared to those with MVD < 14.5 (17.1 months, 95% CI: 12–22.3; log-rank p = 0.037) (Figure 4). Patients in the higher MVD group had a lower hazard of death (HR 0.265, 95% CI 0.070–0.997; p = 0.050) (Table 3). Bootstrap resampling (2000 samples, BCa) supported the stability of this association (bootstrap p = 0.042), with a BCa 95% CI for the HR range of 0.014–0.908). In a multivariable Cox model, MVD ≥ 14.5 was associated with a nonsignificant lower hazard of death (HR: 0.25; 95% CI: 0.08–1.19; p = 0.089) (Table 4). In univariable Cox regression for overall survival

(OS), continuous MVD (per five vessels/HPF at ×400) was not significantly associated with OS (Omnibus score χ^2 = 2.33, df = 1, p = 0.127). The estimated hazard ratio per five-vessel/HPF increase was 0.719 (95% CI 0.468–1.105; p = 0.132) (Table 3).

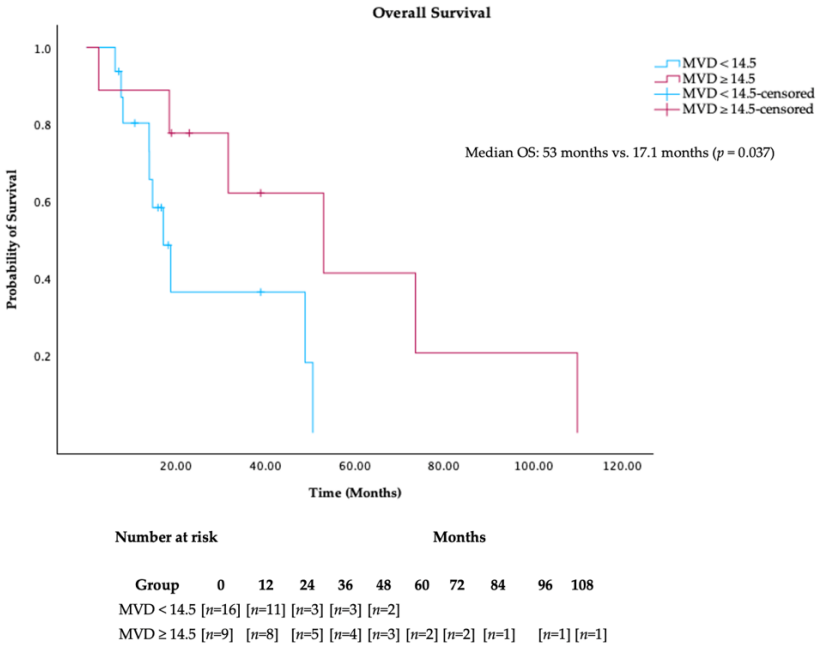


Figure 4. Kaplan–Meier analysis for OS according to MVD subgroups.

Table 3. Univariable Cox regression analysis for OS in derivation cohort.

Variables	Hazard Ratio	*p* Value
MVD Scoring		
≥14.5	0.26 (95% CI: 0.07–0.99)	0.05
<14.5		
Continuous MVD (per 5 vessels/HPF)	0.71 (95% CI: 0.46–1.1)	0.13
Smoking Status		
Smoker	1 (95% CI: 0.32–3.4)	0.94
Non-Smoker		
Gender		
Female	0.41 (95% CI: 0.05–3.2)	0.4
Male		
PD-L1%		
≥1%		0.63
<1%	1.3 (95% CI: 0.43–3.9)	
Age		
≥65	0.28 (95% CI: 0.08–0.93)	0.038
<65		
ECOG Performance		
0		0.51
1	1.5 (95% CI: 0.42–5.5)	
Number of Metastatic Sites		
<2	0.38 (95% CI: 0.13–1)	0.06
≥2		
Brain Metastasis		
Yes	1.4 (95% CI: 0.42–4.6)	0.59
No		
Previous Chemotherapy		
Yes	1.5 (95% CI: 0.46–5)	0.48
No		

Table 4. Multivariable Cox regression analysis for OS in derivation cohort.

Variables	Hazard Ratio	*p* Value
MVD Scoring		
≥14.5	0.25 (95% CI: 0.08–1.19)	0.089
<14.5		
Age		
≥65	0.34 (95% CI: 0.10–1.13)	0.08
<65		

In the derivation cohort, patients with MVD ≥ 14.5 had a significantly longer median TFST (50 months, 95% CI: 1–119.5), compared to those with MVD < 14.5 (6 months, 95% CI: 2.5–9.4; log-rank $p = 0.014$) (Figure 5). High MVD was associated with longer TFST on univariable Cox regression (HR = 0.27; 95% CI: 0.09–0.82; $p = 0.021$; bootstrap $p = 0.031$) (Table 5). In the adjusted model, MVD ≥ 14.5 was associated with a lower hazard for TFST (HR: 0.18; 95% CI: 0.05–0.65; $p = 0.009$) (Table 6).

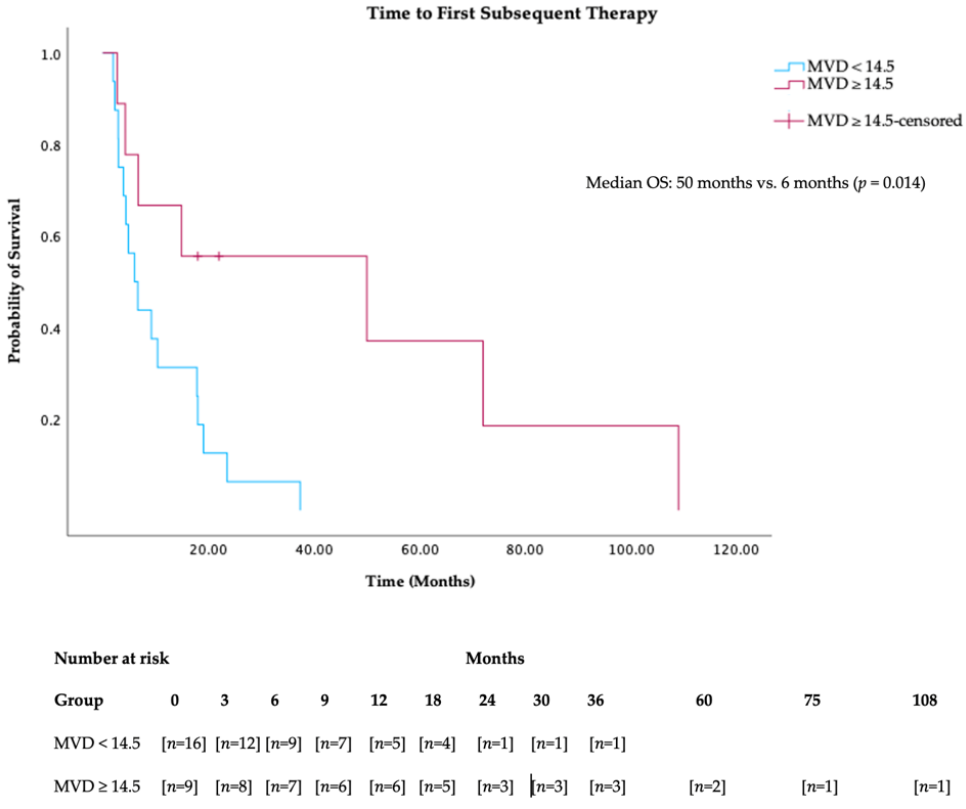


Figure 5. Kaplan–Meier analysis for TFST according to MVD subgroups.

In univariable Cox regression for TFST, continuous MVD (per five vessels/HPF at ×400) was significantly associated with TFST (Omnibus score $\chi^2 = 4.70$, df = 1, $p = 0.030$). Each five-vessel/HPF increase in MVD corresponded to a lower hazard of subsequent therapy (HR 0.663, 95% CI 0.454–0.969; $p = 0.034$) (Table 5). Bootstrap resampling (2000 samples, BCa) supported the robustness of this association (bootstrap $p = 0.032$; BCa 95% CI for HR: 0.44–0.95). In the adjusted model, continuous MVD was associated with a lower hazard for TFST (HR: 0.63; 95% CI: 0.42–0.95; $p = 0.027$) (Table 7). Bootstrap resampling (2000 samples, BCa) supported this association (bootstrap $p = 0.031$; BCa 95% CI for HR:0.31–0.79).

Table 5. Univariable Cox regression analysis for TFST in derivation cohort.

Variables	Hazard Ratio	*p* Value
MVD Scoring		
≥14.5	0.27 (95% CI: 0.08–0.82)	0.021
<14.5		
Continuous MVD (per 5 vessels/HPF)	0.66 (95% CI: 0.45–0.96)	0.034
Smoking Status		
Smoker		0.67
Non-Smoker	1.23 (95% CI: 0.47–3.19)	
Gender		
Female		0.73
Male	1.21 (95% CI: 0.39–3.73)	
PD-L1%		
≥1%		0.28
<1%	1.72 (95% CI: 0.63–4.67)	
Age		
≥65	0.76 (95% CI: 0.31–1.88)	0.56
<65		
ECOG Performance		
0		0.95
1	0.97 (95% CI: 0.37–2.51)	
Number of Metastatic Sites		
<2	0.65 (95% CI: 0.27–1.54)	0.33
≥2		
Brain Metastasis		
Yes	0.88 (95% CI: 0.31–2.47)	0.81
No		
Previous Chemotherapy		
Yes	1.35 (95% CI: 0.53–3.4)	0.51
No		

Table 6. Multivariable Cox regression analysis for TFST in derivation cohort with dichotomized MVD.

Variables	Hazard Ratio	*p* Value
MVD Scoring		
≥14.5	0.18 (95% CI: 0.05–0.65)	0.009
<14.5		
Performance Status		
0	0.44 (95% CI: 0.14–1.36)	0.15
1		

Table 7. Multivariable Cox regression analysis for TFST in derivation cohort with continuous MVD.

Variables	Hazard Ratio	*p* Value
Continuous MVD	0.63 (95% CI: 0.42–0.95)	0.027
Performance Status		
0	0.69 (95% CI: 0.24–1.91)	0.47
1		

To evaluate whether the association between MVD and outcomes differed by treatment type (ICI vs. chemotherapy), formal MVD × treatment interaction terms were tested in logistic regression (ORR) and Cox models (OS and TFST). No statistically significant interaction was observed for ORR, OS, or TFST, indicating that predictive effects could not be confirmed in this dataset. These interaction analyses should be considered exploratory and underpowered.

In the derivation cohort, a parsimonious Cox regression model for TFST including continuous MVD (per five vessels/HPF at ×400) and ICI-treatment line (first-line or subsequent) showed borderline overall fit (Omnibus score $\chi^2 = 5.70$, df = 2, $p = 0.058$). MVD per five vessels/HPF at ×400 was independently associated with longer TFST (HR 0.658 per five-vessel/HPF increase, 95% CI 0.452–0.956; $p = 0.028$), whereas the ICI-treatment line was not significant (HR 1.511, 95% CI 0.598–3.817; $p = 0.383$). Bootstrap resampling (2000 samples, BCa) supported the MVD association (bootstrap $p = 0.047$; BCa 95% CI for an approximate HR range of 0.36–0.86).

A parsimonious Cox regression model for OS including the continuous MVD and ICI-treatment line was not statistically significant overall (Omnibus score $\chi^2 = 3.55$, df = 2, $p = 0.169$). Continuous MVD showed a nonsignificant trend toward improved OS (HR 0.689 per five-vessel/HPF increase, 95% CI 0.447–1.061; $p = 0.091$), and the ICI-treatment line was not significant (HR 1.894, 95% CI 0.561–6.389; $p = 0.304$).

In the pooled cohort (derivation + validation arm), in an exploratory Cox model including MVD group, PD-L1 and their interaction, MVD ≥ 14.5 was associated with longer TFST (HR 0.34, 95% CI 0.12–0.92; $p = 0.035$), while no MVD×PD-L1 interaction was detected ($p = 0.770$), indicating no evidence that the MVD–TFST association differs by PD-L1 category. In the same population, in logistic regression including MVD PD-L1 status and an MVD×PD-L1 interaction term, high MVD was associated with ORR (OR = 0.036, $p = 0.012$). The MVD×PD-L1 interaction was not significant in the primary model ($p = 0.311$), indicating no clear evidence that the MVD–ORR association differs by PD-L1 status. Bootstrap resampling suggested model instability with wide BCa intervals.

In the pooled ICI-treated cohort, a Cox model for TFST including continuous MVD (per five vessels/HPF), PD-L1 status, and an MVD × PD-L1 interaction term was statistically significant overall (Omnibus score $\chi^2 = 12.48$, df = 3, $p = 0.006$). Continuous MVD was independently associated with longer TFST (HR 0.557 per five-vessel/HPF increase; 95% CI 0.359–0.864; $p = 0.009$), whereas PD-L1 showed a nonsignificant association (HR 0.459; 95% CI 0.203–1.041; $p = 0.062$). The MVD × PD-L1 interaction was not significant (HR 1.011; 95% CI 0.540–1.894; $p = 0.973$), indicating no evidence that the MVD–TFST association differs by PD-L1 status. Bootstrap resampling (2000 samples, BCa) supported the robustness of the continuous MVD association (bootstrap $p = 0.002$).

In the pooled ICI-treated cohort, in multivariable logistic regression including the MVD group and ICI-treatment line (first-line or subsequent), high MVD (≥14.5) was associated with markedly lower odds of non-response (OR 0.036; $p = 0.008$), whereas the effect for the ICI-treatment line was not significant ($p = 0.387$).

In the pooled ICI-treated cohort, higher MVD status showed improved TFST (median TFST: 20 months, 95% CI: 3.6–36.3) compared to those with MVD < 14.5 (median TFST: 5 months; 95% CI: 2.5–7.4; log-rank $p = 0.003$) in exploratory analysis. In terms of OS, cases with higher MVD showed a trend towards better outcome (median OS: 31.7 months, 95% CI: 7–56.4), compared to those with MVD < 14.5 (median OS: 14 months, 95% CI: 8.9–19.2, log-rank $p = 0.063$) in the same cohort.

The characteristics of the non-overlapping internal validation cohort (n = 13) are presented in Table 8. In this group, 12 had adenocarcinoma and one case had NSCLC, NOS.

Table 8. The characteristics of the validation cohort (n = 13).

Characteristics	n (%)
Median age (range)	63 (34–77)
Sex	
Male	12 (92.3%)
Female	1 (8.7%)
Smoking Status	
Heavy smoker (≥30 pack-years)	4 (30.7%)
Light smoker (<30 pack-years)	2 (15.3%)
Non-smoker	1 (7.7%)
Missing data	6 (53.8%)
Number of Metastatic Sites	
1 site	9 (69.2%)
2 sites	3 (23%)
3 sites	1 (7.8%)
PD-L1% Status	
1–49%	3 (23%)
≥50%	0
0%	9 (69%)
Missing data	1
Brain Metastasis	
Yes	4 (30.7%)
No	9 (69.3%)
Line of ICI Therapy	
First-line	0
Second-line	13 (100%)
Biopsy Site	
Lung	7 (54%)
Mediastinal lymph nodes	2 (15.3%)
Brain	4 (30.7%)

In the validation cohort (n = 13), the median TFST was 9 months (95% CI: 1–28.4) in cases with MVD ≥ 14.5 vs. 4 months (95% CI: 1.8–6.1) in cases with MVD < 14.5 (log-rank p = 0.035, HR = 0.27 (0.07–1.04)). The median OS was 12 months (95% CI: 1–33.3) in cases with MVD ≥ 14.5 vs. 7 months (95% CI: 4.8–9.1) in those with MVD < 14.5 (log-rank p = 0.059, HR = 0.27 (0.06–1.16)). No significant difference in ORR was observed between MVD subgroups. In the pooled ICI-treated patients, after excluding cases with brain metastasis in the validation cohort, the MVD ≥ 14.5 arm showed a longer TFST (median: 14.9 months; 95% CI: 1–35 vs. median: 4.8 months; 95% CI: 1.4–8.2; log-rank p = 0.012; HR = 0.37 (0.17–0.83)), whereas no significant association with OS was observed. Similarly, in the same group, each five-vessel/HPF increase in MVD corresponded to a lower hazard of subsequent therapy (HR 0.70, 95% CI 0.51–0.94; p = 0.020).

In the chemotherapy-only comparator arm (n = 15), no significant differences in OS or TFST were observed between patients with MVD ≥ 14.5 and those with MVD < 14.5. Similarly, no significant difference in ORR was observed between the higher and lower MVD subgroups. The characteristics of this population are presented in Table 9.

Table 9. The characteristics of the chemotherapy-only comparator arm (n = 15).

Characteristics	n (%)
Median age (range)	61.5 (52–71)
Sex	
Male	14 (93.3%)
Female	1 (7.7%)
Smoking Status	
Heavy smoker (≥30 pack-years)	10 (66.6%)
Light smoker (<30 pack-years)	2 (13.3%)
Non-smoker	1 (6.6%)
Missing data	2 (13.2%)
Number of Metastatic Sites	
1 site	6 (40%)
2 sites	6 (40%)
3 sites	3 (20%)
Brain Metastasis	
Yes	3 (20%)
No	12 (80%)
Biopsy Site	
Lung	9 (60%)
Mediastinal lymph nodes	5 (33.3%)
Brain	1 (6.7%)

4. Discussion

This observational study evaluated the impact of MVD score on ICI efficacy in patients with metastatic non-squamous non-small cell lung cancer and suggested that increased CD34-stained MVD might be associated with improved outcome.

The dynamic TME has been explored to predict ICI efficacy in lung cancer [13,14,16,17,23]. Co-occurring genomic alterations (e.g., STK11/KEAP1), less common driver mutations, tumor immune-evasion mechanisms and even smoking history may affect immune phenotypes that alter ICI efficacy [13–15,17,21,46]. Emerging data indicate that these determinants often exert their effect on vascular and metabolic components of TME including hypoxia, immune cell trafficking, antigen presentation, and effector T-cell function [13,15,17,21,23,46].

VEGF-mediated tumor angiogenesis produces fragile non-functioning vessels that precede immune cell infiltration, foster hypoxia, and promote the accumulation of immunosuppressive cells [17,18,24–26]. Elevated VEGF levels are linked to tumor progression and distant metastasis, thereby triggering tumor immune escape mechanisms with impaired immune cell functions [15,18,24–26].

Vessel normalization indicates a shift toward functionally competent, pericyte-covered microvessels that improve perfusion, nutrient and oxygen delivery, and restore endothelial adhesion molecules, thereby facilitating immune cell infiltration [30,31,36,37]. Preclinical studies have shown that vessel normalization may enhance antitumor response and improve the efficacy of ICIs [36,37]. In our study, MVD was assessed using CD34 alone, without evaluation of pericyte coverage or perfusion. Therefore, vascular normalization could not be defined properly. Better ICI outcomes associated with higher CD34-stained MVD may be interpreted as being consistent with a more permissive vascular bed that facilitates the trafficking of antitumoral immune cells. As a practical IHC measure, CD34-stained MVD may help contextualize the benefit of ICIs in relation to vascular structure.

In this study, the 14.5 vessel/HPF cut-off was derived to provide a clinically interpretable stratification and was applied without re-optimization to the non-overlapping internal validation cohort. Internal resampling validation of the ROC-derived Youden

cut-point was not performed; therefore, the 14.5 vessel/HPF threshold should be considered exploratory.

Given the continuous nature of microvessel density, we evaluated MVD not only using the ROC-derived threshold but also as a continuous predictor. This cut-off-independent approach mitigates concerns that findings are driven by data-derived dichotomization. In these analyses, higher MVD remained associated with longer TFST, supporting that the observed signal is not solely dependent on the 14.5 cut-off.

Because PD-L1 data were missing in a subset of patients, PD-L1-adjusted analyses were performed as sensitivity analyses in the pooled ICI-treated cohort. In these models, higher MVD (for both dichotomized and continuous) remained associated with TFST, while PD-L1 was not statistically significant. In addition, formal MVD×PD-L1 interaction testing did not demonstrate effect modification, suggesting that the association between MVD and TFST does not differ by PD-L1 category in this dataset. These findings support that MVD might capture information not fully explained by PD-L1, while acknowledging limitations due to missingness and its exploratory nature.

In this study, although an observational chemotherapy-only comparator cohort was included, the comparator sample was limited. Formal treatment–biomarker interaction testing did not confirm an MVD $\times$ treatment interaction for ORR, TFST, or OS. Therefore, our results should not be interpreted as establishing MVD as a definitive predictive biomarker.

Our study has limitations. Given the small sample size, our findings should be considered hypothesis-generating. The small sample size and limited number of events for survival analyses may have increased the risk of unstable HR values with wide-range confidence intervals. Therefore, multivariable models were kept parsimonious, and robustness was evaluated using bootstrap resampling.

The validation cohort comprised heterogeneous specimen sources reflecting real-world sampling for diagnosis and staging. Survival was shorter in the validation cohort than in the derivation cohort, potentially due to a higher prevalence of brain metastases and the fact that all validation cases received ICI in the second-line setting. Also in derivation cohort, many patients received ICI in the second-line setting because during the earlier period of the study, ICIs were commonly administered after progression of chemotherapy, whereas later, ICIs became the first-line standard of care. This temporal shift contributed to line-of-therapy heterogeneity. Although it was exploratory, in the pooled ICI-treated cohort (including more second-line cases), higher MVD remained associated with longer TFST in both categorical (MVD $\geq$ 14.5) and continuous models, supporting that the observed association is not driven solely by treatment line setting.

In the derivation cohort, we included specimens obtained from both lung and lymph nodes. Although these tissues differ anatomically and histologically, the analysis was limited to tumor deposits in each specimen. Nevertheless, intratumoral vascular heterogeneity may have affected MVD assessment. In addition, although the supplementary analysis excluding cases with brain metastases demonstrated similar results, this does not fully address the potential effect of biopsy-site-related vascular heterogeneity. Therefore, residual uncertainty related to anatomical site differences should be kept in mind when interpreting the findings.

Since the best assessment tool to define MVD is not clear, our results could have been validated with additional markers such as anti-CD31 antibodies, VEGF, and also by integrating vascular normalization markers (e.g., pericyte markers such as alpha-SMA/NG2).

Finally, economic implications of assessing MVD should be considered. Although CD34-stained MVD measurement may incur additional expenses as digital pathology resources for quantification and increased workload for pathologists, it is still relatively low-cost compared with more complex molecular assays (e.g., next-generation sequencing).

Also, with validation in prospective larger studies, quantification of MVD might identify patients who will likely derive benefit from ICIs, thereby enhancing the cost-effectiveness of immunotherapy.

Despite these limitations, this study provides preliminary evidence that CD34-stained MVD may serve as a vascular metric associated with improved ICI efficacy in advanced non-squamous NSCLC. Especially given the recent publications regarding the role of Ivonescimab—a bispecific antibody against PD-1 and VEGF—in metastatic NSCLC [45,46], further investigations in this area may be warranted.

5. Conclusions

Higher CD34-MVD may be a feasible vascular metric associated with ICI outcomes in metastatic non-squamous NSCLC that warrants prospective validation.

Author Contributions: Conceptualization, E.C. and Z.H.T.; methodology, E.O. and A.T.; software, E.O.; validation, S.B., C.Y. and A.B.Ö.; investigation, E.C. and Z.H.T.; resources, S.B., C.Y. and A.B.Ö.; data curation, S.B., C.Y. and A.B.Ö.; writing—original draft preparation, E.C.; writing—review and editing, Z.H.T.; supervision, Z.H.T.; project administration, Z.H.T. All authors have read and agreed to the published version of the manuscript.

Funding: This research was funded by Istanbul University-Cerrahpasa Scientific Research Projects Department (Project ID number: 34995).

Institutional Review Board Statement: The study was conducted in accordance with the Declaration of Helsinki and approved by the Clinical Research Ethics Committee of Istanbul University-Cerrahpasa Faculty of Medicine (ID: 89403766-604.01.02.9846, approval date 6 March 2025) for studies involving humans.

Informed Consent Statement: An informed consent form was deemed unnecessary according to the Clinical Research Committee of Istanbul University-Cerrahpasa Faculty of Medicine (ID: 89403766-604.01.02.9846) for studies involving humans.

Data Availability Statement: The raw data supporting the conclusions of this article will be made available by the authors on request.

Conflicts of Interest: The authors declare no conflicts of interest. The funders had no role in the design of the study; in the collection, analyses, or interpretation of data; in the writing of the manuscript; or in the decision to publish the results.

Abbreviations

ALK	Anaplastic Lymphoma Kinase
AUC	Area Under the Curve
CI	Confidence Interval
CT	Computed Tomography
DAB	Diaminobenzidine Tetrahydrochloride
EGFR	Epidermal Growth Factor Receptor
FDG PET CT	Fluorodeoxyglucose Positron Emission Tomography
FFPE	Formalin-fixed Paraffin-embedded
FNA	Fine Needle Aspiration
HPF	High-power Field
HR	Hazard Ratio
ICI	Immune Checkpoint Inhibitor
IHC	Immunohistochemistry
MDSC	Myeloid-derived Suppressor Cell
MVD	Microvessel Density
NSCLC	Non-small Cell Lung Cancer

ORR	Objective Response Rate
OS	Overall Survival
PBS	Phosphate-Buffered Saline
PD-1	Programmed Cell Death Protein 1
PD-L1	Programmed Death Ligand-1
PIGF	Placental Growth Factor
RECIST	Response Evaluation Criteria in Solid Tumors
ROC	Receiver Operating Characteristic
TFST	Time to First Subsequent Therapy
TME	Tumor Microenvironment
VEGF	Vascular Endothelial Growth Factor

References

1. Molina, J.R.; Yang, P.; Cassivi, S.D.; Schild, S.E.; Adjei, A.A. Non-small cell lung cancer: Epidemiology, risk factors, treatment, and survivorship. *Mayo Clin. Proc.* **2008**, *83*, 584–594. [CrossRef]
2. Wu, Z.; Yibulayin, W.; He, D.; Xu, K.; Yibulayin, X.; Ma, L.; Sun, X. EGFR and K-Ras Gene Mutations in the Diagnosis of Non-Small Cell Lung Cancer and their Pathological Correlation. *Int. J. Pharmacol.* **2024**, *20*, 874–882. [CrossRef]
3. Borghaei, H.; Paz-Ares, L.; Horn, L.; Spigel, D.R.; Steins, M.; Ready, N.E.; Chow, L.Q.; Vokes, E.E.; Felip, E.; Holgado, E. Nivolumab versus docetaxel in advanced nonsquamous non–small-cell lung cancer. *N. Engl. J. Med.* **2015**, *373*, 1627–1639. [CrossRef] [PubMed]
4. Garon, E.B.; Rizvi, N.A.; Hui, R.; Leighl, N.; Balmanoukian, A.S.; Eder, J.P.; Patnaik, A.; Aggarwal, C.; Gubens, M.; Horn, L. Pembrolizumab for the treatment of non–small-cell lung cancer. *N. Engl. J. Med.* **2015**, *372*, 2018–2028. [CrossRef]
5. Herbst, R.S.; Giaccone, G.; de Marinis, F.; Reinmuth, N.; Vergnenegre, A.; Barrios, C.H.; Morise, M.; Felip, E.; Andric, Z.; Geater, S. Atezolizumab for first-line treatment of PD-L1–selected patients with NSCLC. *N. Engl. J. Med.* **2020**, *383*, 1328–1339. [CrossRef]
6. Gandhi, L.; Rodríguez-Abreu, D.; Gadgeel, S.; Esteban, E.; Felip, E.; De Angelis, F.; Domine, M.; Clingan, P.; Hochmair, M.J.; Powell, S.F. Pembrolizumab plus chemotherapy in metastatic non–small-cell lung cancer. *N. Engl. J. Med.* **2018**, *378*, 2078–2092. [CrossRef] [PubMed]
7. Paz-Ares, L.; Ciuleanu, T.-E.; Cobo, M.; Schenker, M.; Zurawski, B.; Menezes, J.; Richardet, E.; Bennouna, J.; Felip, E.; Juan-Vidal, O. First-line nivolumab plus ipilimumab combined with two cycles of chemotherapy in patients with non-small-cell lung cancer (CheckMate 9LA): An international, randomised, open-label, phase 3 trial. *Lancet Oncol.* **2021**, *22*, 198–211, Correction in *Lancet Oncol.* **2021**, *22*, E92. [CrossRef]
8. Barlesi, F.; Vansteenkiste, J.; Spigel, D.; Ishii, H.; Garassino, M.; de Marinis, F.; Özgüroğlu, M.; Szczesna, A.; Polychronis, A.; Uslu, R. Avelumab versus docetaxel in patients with platinum-treated advanced non-small-cell lung cancer (JAVELIN Lung 200): An open-label, randomised, phase 3 study. *Lancet Oncol.* **2018**, *19*, 1468–1479, Correction in *Lancet Oncol.* **2018**, *19*, E581. [CrossRef]
9. Brahmer, J.R.; Lee, J.-S.; Ciuleanu, T.-E.; Bernabe Caro, R.; Nishio, M.; Urban, L.; Audigier-Valette, C.; Lupinacci, L.; Sangha, R.; Pluzanski, A. Five-year survival outcomes with nivolumab plus ipilimumab versus chemotherapy as first-line treatment for metastatic non–small-cell lung cancer in CheckMate 227. *J. Clin. Oncol.* **2023**, *41*, 1200–1212. [CrossRef] [PubMed]
10. Garassino, M.C.; Gadgeel, S.; Speranza, G.; Felip, E.; Esteban, E.; Dómine, M.; Hochmair, M.J.; Powell, S.F.; Bischoff, H.G.; Peled, N. Pembrolizumab plus pemetrexed and platinum in nonsquamous non–small-cell lung cancer: 5-year outcomes from the phase 3 KEYNOTE-189 study. *J. Clin. Oncol.* **2023**, *41*, 1992–1998. [CrossRef]
11. Brahmer, J.R.; Lacchetti, C.; Schneider, B.J.; Atkins, M.B.; Brassil, K.J.; Caterino, J.M.; Chau, I.; Ernstoff, M.S.; Gardner, J.M.; Ginex, P. Management of immune-related adverse events in patients treated with immune checkpoint inhibitor therapy: American Society of Clinical Oncology Clinical Practice Guideline. *J. Clin. Oncol.* **2018**, *36*, 1714–1768. [CrossRef]
12. Meyer, M.-L.; Fitzgerald, B.G.; Paz-Ares, L.; Cappuzzo, F.; Jaenne, P.A.; Peters, S.; Hirsch, F.R. New promises and challenges in the treatment of advanced non-small-cell lung cancer. *Lancet* **2024**, *404*, 803–822. [CrossRef]
13. Passaro, A.; Brahmer, J.; Antonia, S.; Mok, T.; Peters, S. Managing resistance to immune checkpoint inhibitors in lung cancer: Treatment and novel strategies. *J. Clin. Oncol.* **2022**, *40*, 598–610. [CrossRef]
14. Albini, A.; Bruno, A.; Noonan, D.M.; Mortara, L. Contribution to tumor angiogenesis from innate immune cells within the tumor microenvironment: Implications for immunotherapy. *Front. Immunol.* **2018**, *9*, 527. [CrossRef] [PubMed]
15. Chen, D.S.; Mellman, I. Oncology meets immunology: The cancer-immunity cycle. *Immunity* **2013**, *39*, 1–10. [CrossRef] [PubMed]
16. Kim, J.; Chen, D.S. Immune escape to PD-L1/PD-1 blockade: Seven steps to success (or failure). *Ann. Oncol.* **2016**, *27*, 1492–1504. [CrossRef] [PubMed]
17. Voron, T.; Colussi, O.; Marcheteau, E.; Pernot, S.; Nizard, M.; Pointet, A.-L.; Latreche, S.; Bergaya, S.; Benhamouda, N.; Tanchot, C. VEGF-A modulates expression of inhibitory checkpoints on CD8+ T cells in tumors. *J. Exp. Med.* **2015**, *212*, 139–148. [CrossRef]

18. Chen, D.S.; Irving, B.A.; Hodi, F.S. Molecular pathways: Next-generation immunotherapy—Inhibiting programmed death-ligand 1 and programmed death-1. *Clin. Cancer Res.* **2012**, *18*, 6580–6587. [CrossRef]
19. Creelan, B.C. Update on immune checkpoint inhibitors in lung cancer. *Cancer Control.* **2014**, *21*, 80–89. [CrossRef]
20. Duan, J.; Wang, Y.; Jiao, S. Checkpoint blockade-based immunotherapy in the context of tumor microenvironment: Opportunities and challenges. *Cancer Med.* **2018**, *7*, 4517–4529. [CrossRef]
21. Murdoch, C.; Muthana, M.; Coffelt, S.B.; Lewis, C.E. The role of myeloid cells in the promotion of tumour angiogenesis. *Nat. Rev. Cancer* **2008**, *8*, 618–631. [CrossRef]
22. Rahma, O.E.; Hodi, F.S. The intersection between tumor angiogenesis and immune suppression. *Clin. Cancer Res.* **2019**, *25*, 5449–5457. [CrossRef]
23. Bremnes, R.M.; Camps, C.; Sirera, R. Angiogenesis in non-small cell lung cancer: The prognostic impact of neoangiogenesis and the cytokines VEGF and bFGF in tumours and blood. *Lung Cancer* **2006**, *51*, 143–158. [CrossRef]
24. Yano, T.; Tanikawa, S.; Fujie, T.; Masutani, M.; Horie, T. Vascular endothelial growth factor expression and neovascularisation in non-small cell lung cancer. *Eur. J. Cancer* **2000**, *36*, 601–609. [CrossRef]
25. Greenberg, J.I.; Shields, D.J.; Barillas, S.G.; Acevedo, L.M.; Murphy, E.; Huang, J.; Scheppke, L.; Stockmann, C.; Johnson, R.S.; Angle, N. A role for VEGF as a negative regulator of pericyte function and vessel maturation. *Nature* **2008**, *456*, 809–813. Erratum in *Nature* **2009**, *457*, 1168. [CrossRef] [PubMed]
26. Macchiarini, P.; Fontanini, G.; Squartini, F.; Angeletti, C.; Hardin, M. Relation of neovascularisation to metastasis of non-small-cell lung cancer. *Lancet* **1992**, *340*, 145–146. [CrossRef]
27. Carmeliet, P.; Jain, R.K. Principles and mechanisms of vessel normalization for cancer and other angiogenic diseases. *Nat. Rev. Drug Discov.* **2011**, *10*, 417–427. [CrossRef] [PubMed]
28. Huang, Y.; Goel, S.; Duda, D.G.; Fukumura, D.; Jain, R.K. Vascular normalization as an emerging strategy to enhance cancer immunotherapy. *Cancer Res.* **2013**, *73*, 2943–2948. [CrossRef]
29. Rolny, C.; Mazzone, M.; Tugues, S.; Laoui, D.; Johansson, I.; Coulon, C.; Squadrito, M.L.; Segura, I.; Li, X.; Knevels, E. HRG inhibits tumor growth and metastasis by inducing macrophage polarization and vessel normalization through downregulation of PlGF. *Cancer Cell* **2011**, *19*, 31–44. [CrossRef]
30. Lee, W.S.; Yang, H.; Chon, H.J.; Kim, C. Combination of anti-angiogenic therapy and immune checkpoint blockade normalizes vascular-immune crosstalk to potentiate cancer immunity. *Exp. Mol. Med.* **2020**, *52*, 1475–1485. [CrossRef] [PubMed]
31. Xiao, M.; Shi, Y.; Jiang, S.; Cao, M.; Chen, W.; Xu, Y.; Xu, Z.; Wang, K. Recent advances of nanomaterial-based anti-angiogenic therapy in tumor vascular normalization and immunotherapy. *Front. Oncol.* **2022**, *12*, 1039378. [CrossRef]
32. Fan, P.; Zhang, N.; Candi, E.; Agostini, M.; Piacentini, M.; TOR Centre; Shi, Y.; Huang, Y.; Melino, G. Alleviating hypoxia to improve cancer immunotherapy. *Oncogene* **2023**, *42*, 3591–3604. [CrossRef] [PubMed]
33. Luo, X.; Zou, W.; Wei, Z.; Yu, S.; Zhao, Y.; Wu, Y.; Wang, A.; Lu, Y. Inducing vascular normalization: A promising strategy for immunotherapy. *Int. Immunopharmacol.* **2022**, *112*, 109167. [CrossRef] [PubMed]
34. Li, W.; Quan, Y.-Y.; Li, Y.; Lu, L.; Cui, M. Monitoring of tumor vascular normalization: The key points from basic research to clinical application. *Cancer Manag. Res.* **2018**, *10*, 4163–4172. [CrossRef]
35. Mineo, T.; Ambrogi, V.; Baldi, A.; Rabitti, C.; Bollero, P.; Vincenzi, B.; Tonini, G. Prognostic impact of VEGF, CD31, CD34, and CD105 expression and tumour vessel invasion after radical surgery for IB–IIA non-small cell lung cancer. *J. Clin. Pathol.* **2004**, *57*, 591–597. [CrossRef] [PubMed]
36. Offersen, B.V.; Pfeiffer, P.; Hamilton-Dutoit, S.; Overgaard, J. Patterns of angiogenesis in nonsmall-cell lung carcinoma. *Cancer Interdiscip. Int. J. Am. Cancer Soc.* **2001**, *91*, 1500–1509. [CrossRef]
37. Trivella, M.; Pezzella, F.; Pastorino, U.; Harris, A.L.; Altman, D.G. Microvessel density as a prognostic factor in non-small-cell lung carcinoma: A meta-analysis of individual patient data. *Lancet Oncol.* **2007**, *8*, 488–499. Erratum in *Lancet Oncol.* **2007**, *8*, 670. [CrossRef]
38. Meert, A.-P.; Paesmans, M.; Martin, B.; Delmotte, P.; Berghmans, T.; Verdebout, J.-M.; Lafitte, J.-J.; Mascaux, C.; Sculier, J.-P. The role of microvessel density on the survival of patients with lung cancer: A systematic review of the literature with meta-analysis. *Br. J. Cancer* **2002**, *87*, 694–701. [CrossRef]
39. Vermeulen, P.; Gasparini, G.; Fox, S.; Colpaert, C.; Marson, L.; Gion, M.; Beliën, J.; De Waal, R.; Van Marck, E.; Magnani, E. Second international consensus on the methodology and criteria of evaluation of angiogenesis quantification in solid human tumours. *Eur. J. Cancer* **2002**, *38*, 1564–1579. [CrossRef]
40. Matsuyama, K.; Chiba, Y.; Sasaki, M.; Tanaka, H.; Muraoka, R.; Tanigawa, N. Tumor angiogenesis as a prognostic marker in operable non–small cell lung cancer. *Ann. Thorac. Surg.* **1998**, *65*, 1405–1409. [CrossRef]
41. Cox, G.; Walker, R.; Andi, A.; Steward, W.; O'Byrne, K.J. Prognostic significance of platelet and microvessel counts in operable non-small cell lung cancer. *Lung Cancer* **2000**, *29*, 169–177. [CrossRef] [PubMed]
42. Qiu, Z.; Wu, J.; Pang, G.; Xu, X.; Lin, J.; Wang, P. CD34 evaluation of microvasculature in lung adenocarcinoma and its microvascular density predicts postoperative tumor recurrence. *Pathol. Oncol. Res.* **2025**, *31*, 1611985. [CrossRef] [PubMed]

43. Sanborn, R.E.; Schneiders, F.L.; Senan, S.; Gadgeel, S.M. Beyond checkpoint inhibitors: Enhancing antitumor immune response in lung cancer. *Am. Soc. Clin. Oncol. Educ. Book* **2022**, *42*, 673–686. [CrossRef]
44. Young, P.E.; Baumhueter, S.; Lasky, L.A. The sialomucin CD34 is expressed on hematopoietic cells and blood vessels during murine development. *Blood* **1995**, *85*, 96–105. [CrossRef]
45. Zhou, C.; Chen, J.; Wu, L.; Wang, L.; Xiong, A.; Liu, B.; Yao, J.; Zhong, H.; Li, J.; Cheng, Y. Phase 3 Study of Ivonescimab (AK112) vs. Pembrolizumab as First-line Treatment for PD-L1-positive Advanced NSCLC: HARMONi-2. In Proceedings of the 2024 World Conference on Lung Cancer, San Diego, CA, USA, 7–10 September 2024.
46. Fang, W.; Zhao, Y.; Luo, Y.; Yang, R.; Huang, Y.; He, Z.; Zhao, H.; Li, M.; Li, K.; Song, Q. Ivonescimab plus chemotherapy in non–small cell lung cancer with EGFR variant: A randomized clinical trial. *JAMA* **2024**, *332*, 561–570. [PubMed]

Disclaimer/Publisher's Note: The statements, opinions and data contained in all publications are solely those of the individual author(s) and contributor(s) and not of MDPI and/or the editor(s). MDPI and/or the editor(s) disclaim responsibility for any injury to people or property resulting from any ideas, methods, instructions or products referred to in the content.